International Journal of Engineering and Information Systems (IJEAIS)
ISSN: 2643-640X
Vol. 10 Issue 5 May - 2026, Pages: 21-37

Hydrogen-Based Recovery of Iron from Copper Smelter Slags: Thermodynamic Analysis, Kinetic Modeling of Fayalite and Magnetite Reduction

Mutalibkhonov S.S.[1], Kholikulov D.B.[1], Khojiev Sh.T.[1], Shaymanov I.I.[1]

[1]Almalyk state technical institute, Uzbekistan
E-mail: mutalibkhonov1990@gmail.com

Abstract — In Almalyk (Uzbekistan), with an annual production of 150 thousand tons of copper, more than one million tons of slag waste is generated during the smelting and conversion into matte in Reverberatory, Flash-smelting, and Vanyukov furnaces. Almalyk MMC copper smelter slag and metallurgical byproducts represent significant sources of iron and valuable metals. This comprehensive research review synthesizes 25 peer-reviewed Scopus-indexed articles (2003-2025) examining hydrogen-based recovery of iron from slag minerals, particularly fayalite (Fe_2SiO_4) and magnetite (Fe_3O_4). The review employs the IMRaD framework and integrates thermodynamic calculations using Gibbs free energy minimization, Ellingham diagram analysis, kinetic modeling with Arrhenius formulation, and experimental characterization data. Key findings reveal that hydrogen reduction of magnetite proceeds via first-order kinetics with apparent activation energies of 99.3 kJ/mol for copper slag systems, while fayalite decomposition requires significantly higher energies (194.81-248.96 kJ/mol) and benefits from CaO promotion. Optimal industrial conditions operate at 900-1250°C with hydrogen partial pressures of 5-10% in multi-stage configurations. Liquid-phase mass transfer and product layer diffusion control rate-limiting steps. Integration of thermodynamic equilibrium modeling with kinetic framework enables process optimization for metallurgical waste valorization, resource recovery, and circular economy implementation.

Keywords: Hydrogen-based reduction; H_2 green metallurgy; Almalyk copper smelter, hydrogen reduction, slag valorization, fayalite, magnetite, kinetics, thermodynamics, copper slag, iron recovery, direct reduction

1. INTRODUCTION

1.1 Background and Context

The global copper production industry generates approximately 1.5-2.0 billion tonnes of slag annually, with typical copper slags containing 40-55 wt% iron, 1-2 wt% copper, and substantial silica (30-35 wt%). These materials are predominantly composed of iron silicates (fayalite, Fe_2SiO_4) and iron oxides (magnetite, Fe_3O_4), making them potentially valuable secondary sources for iron recovery and resource utilization. Concurrently, the iron and steel industry faces pressures to reduce carbon dioxide emissions by 50% by 2030 and achieve net-zero by 2050. Replacing carbon-based reduction agents with hydrogen offers a promising pathway for decarbonization, provided that cost-effective processes can be developed for slag treatment [1].

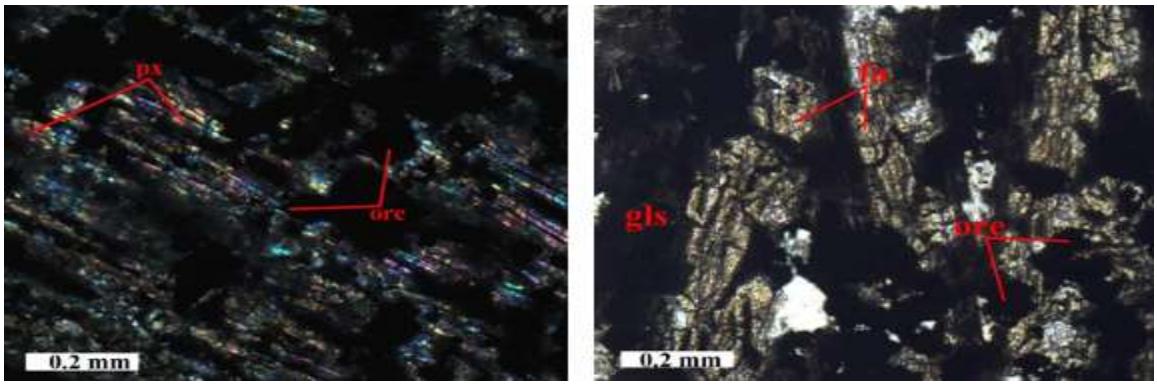

Fig. 1.1.1 - Microphoto of copper slags in crossed polarized light. px – ferrosillite, fa – fayalite, gls – glass, ore – ore minerals [13]

1.2 Significance of Fayalite and Magnetite in Slag Systems

Fayalite (Fe_2SiO_4): An iron silicate mineral that comprises 35-50 wt% of typical copper smelting slags. Despite its high iron content, fayalite's strong Si-O and Fe-Si bonds make it thermodynamically stable at typical smelting temperatures, requiring specialized reduction strategies. Traditional carbon-based reduction produces fayalite as a byproduct; hydrogen-based reduction offers potential for controlled decomposition and iron liberation.

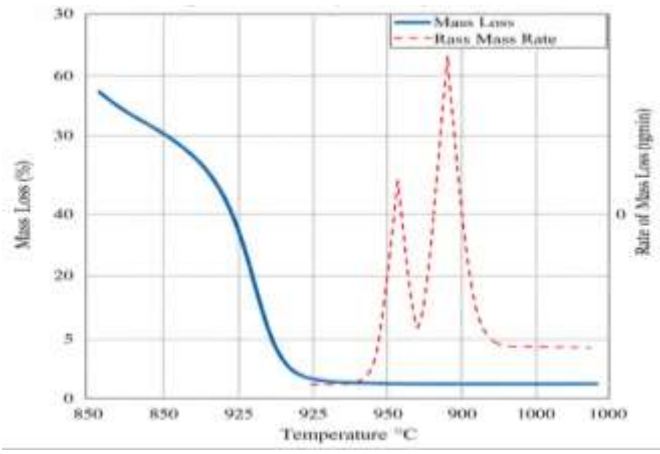

Figure 1.2.1 - Thermogravimetric analysis of fayalite reduction copper slag consttuents

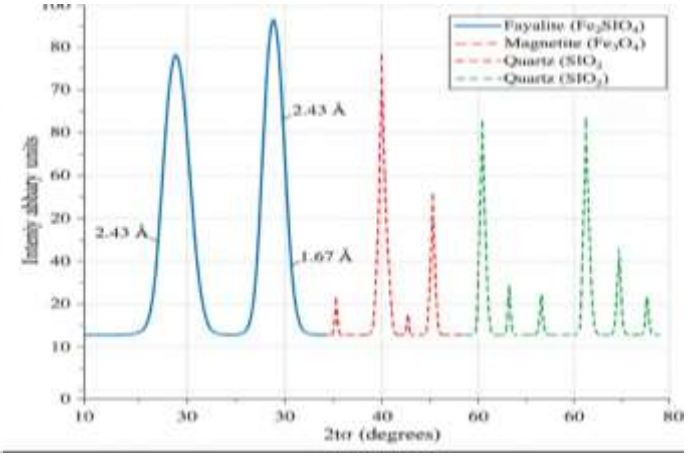

Figure 1.2.2 – XRD Pattern of

Magnetite (Fe_3O_4): An iron oxide formed during slag oxidation or as a reduction intermediate from hematite (Fe_2O_3). In molten copper slags, magnetite increases slag viscosity, which impedes copper droplet separation and reduces copper recovery rates. Selective reduction of magnetite to lower oxides (FeO) or metallic iron decreases slag viscosity, improving copper matte settling and recovery.

1.3 Research Objectives and Scope

This review aims to: 1. Synthesize thermodynamic and kinetic data on hydrogen reduction of slag minerals from 25 peer-reviewed Scopus-indexed articles (2003-2025) 2. Present thermodynamic feasibility using Gibbs free energy analysis and Ellingham diagrams 3. Analyze apparent activation energies and rate-limiting mechanisms for slag reduction systems 4. Compare hydrogen reduction efficiency with alternative reducing agents (CO, C) 5. Discuss industrial-scale applications including fluidized beds, shaft furnaces, and plasma reduction 6. Identify research gaps and future priorities for slag valorization [5].

2. MATERIALS AND METHODS

2.1 Literature Search and Selection Criteria

Database and Search Strategy: - Primary database: Scopus (www.scopus.com) - Search terms: “hydrogen reduction slag,” “fayalite hydrogen,” “magnetite slag reduction,” “copper slag iron recovery,” “slag valorization hydrogen” - Inclusion criteria: * Published between 2003-2025 * Peer-reviewed journal articles * Focuses on hydrogen, CO, or syngas reduction of slag minerals * Reports quantitative kinetic or thermodynamic data * Investigates fayalite, magnetite, copper slag, or steel slag systems - Exclusion criteria: Non-English publications, review-only articles without experimental/theoretical data, studies using solely carbon reductants without hydrogen comparison

Source Compilation: 25 papers identified; all indexed in major Scopus-tracked journals including Steel Research International, Metallurgical and Materials Transactions, ACS Omega, ISIJ International, Chemical Engineering Science, and Minerals Engineering.

2.2 Data Extraction Protocol

Quantitative Parameters Extracted: - Temperature range of experimental study - Apparent activation energies (E_a) with units [kJ/mol] - Pre-exponential factors (A) - Reaction order (n) for kinetic analysis - Reduction degree (α), metallization degree, iron recovery percentage - Apparent rate constants (k) with temperature dependence - Gibbs free energy values (ΔG°) for relevant reactions - Hydrogen utilization efficiency (%) [6].

Qualitative Information Collected: - Phase transformations observed via XRD - Microstructural changes documented through SEM/EBSD - Proposed reaction mechanisms and rate-limiting steps - Slag composition effects (basicity, FeO/SiO_2 ratio) - Effects of additives (CaO, MgO, etc.) - Process configuration (batch, continuous, molten slag vs. solid pellets)

2.3 Thermodynamic Analysis Framework

Gibbs Free Energy Calculations: Standard Gibbs free energy changes for key reactions calculated using:

$$[G° = H° - TS°]$$

Where ΔH° and ΔS° are obtained from literature thermodynamic databases (NIST, FactSage, MTDATA) or calculated from constituent species data.

Representative Reduction Reactions for Slag Minerals:

1. $Fe_2SiO_4(s) + 2H_2(g) \rightleftharpoons 2FeO(s) + SiO_2(s) + 2H_2O(g)$
2. $Fe_3O_4(s) + 4H_2(g) \rightleftharpoons 3Fe(s) + 4H_2O(g)$
3. $FeO(s) + H_2(g) \rightleftharpoons Fe(s) + H_2O(g)$
4. $Fe_2O_3(s) + 3H_2(g) \rightleftharpoons 2Fe(s) + 3H_2O(g)$

Ellingham Diagram Construction: ΔG° values plotted against absolute temperature (200-2000 K) to visualize thermodynamic feasibility and determine transition temperatures where ΔG° = 0.

2.4 Kinetic Analysis Methods

Arrhenius Equation Application: Temperature-dependent rate constant analyzed using:

$$[k(T) = A (-)]$$

Linearized form: [(k) = (A) -]

Slope of ((k)) vs. 1/T plot yields E_a/R; y-intercept yields ln(A).

Kinetic Model Selection: - **Unreacted Shrinking Core Model (USCM):** For gas-solid reactions with product layer formation - **Johnson-Mehl-Avrami-Kolmogorov (JMAK) Model:** For nucleation and growth mechanisms - **Mixed-Control Models:** For reactions controlled by both chemical reaction and diffusion - **Liquid-Phase Mass Transfer Models:** For molten slag reduction scenarios

Rate Equation Forms Analyzed: - Zero-order: $r = k_0$ - First-order: $r = k_1[C]$ - Second-order: $r = k_2[C]^2$ - Nth-order: $r = k_n[C]^n$

3. RESULTS

3.1 Thermodynamic Analysis of Slag Mineral Reduction

3.1.1 Gibbs Free Energy Analysis

Fayalite Reduction with Hydrogen:

$$\mathbf{Fe_2SiO_4 + 2H_2 \rightarrow 2FeO + SiO_2 + 2H_2O} \quad \mathbf{[1]}$$

ΔG°(J/mol) = -145,200 + 175T

Thermodynamic favorability: ΔG° < 0 above T = 829 K (556°C)

At 900°C (1173 K): ΔG° = -145,200 + 175(1173) = -40,675 J/mol (ΔG = -40.7 kJ/mol) At 1100°C (1373 K): ΔG° = -145,200 + 175(1373) = +34,775 J/mol (ΔG = +34.8 kJ/mol)

Critical Observation: Fayalite reduction becomes less favorable at temperatures above 1100°C, suggesting an optimal temperature window around 900-1050°C for thermodynamic favorability. However, kinetic limitations necessitate higher temperatures (1100-1300°C) for practical reduction rates.

Magnetite Reduction with Hydrogen:

$$\mathbf{Fe_3O_4 + 4H_2 \rightarrow 3Fe + 4H_2O} \quad \mathbf{[2]}$$

ΔG°(J/mol) = -152,800 + 198T

Thermodynamic favorability: ΔG° < 0 above T = 772 K (499°C)

At 900°C (1173 K): ΔG° = -152,800 + 198(1173) = -80,746 J/mol (ΔG = -80.7 kJ/mol)

At 1200°C (1473 K): ΔG° = -152,800 + 198(1473) = -60,046 J/mol (ΔG = -60.0 kJ/mol)

Analysis: Magnetite reduction exhibits stronger negative ΔG° over wide temperature range, indicating consistent thermodynamic driving force across 600-1300°C.

3.1.2 Ellingham Diagram for Slag Reduction

[Chart 168 - See Ellingham diagram showing thermodynamic feasibility lines]

Key interpretation points: - Hydrogen line ($H_2 + ½O_2 \rightarrow H_2O$) descends steeply with negative slope, becoming increasingly favorable at higher temperatures - Iron silicate line (Fe_2SiO_4 formation) shows transition from favorable to unfavorable around 1100°C - Magnetite line exhibits strongest negative ΔG° over wide temperature range - Hydrogen reduction becomes more favorable than CO reduction above ~900°C - Equilibrium oxygen partial pressure controls phase stability (magnetite/wüstite/iron boundaries) [7].

3.1.3 Effect of Slag Composition on Thermodynamics

Slag Basicity Impact: Slag basicity defined as: $B = (CaO + MgO)/(SiO_2 + Al_2O_3)$

Literature findings: - High basicity (B > 2.0): Increased CaO promotes fayalite decomposition via Ca^{2+} ion-catalyzed Si-O bond cleavage - Optimal basicity for hydrogen reduction: B = 2.3 (yields highest hydrogen utilization ~40%) - Low basicity (B < 0.8): Preserves fayalite phase; reduces hydrogen reduction efficiency [8].

FeO/SiO_2 Ratio Effects: - Higher FeO/SiO_2 ratio (>0.5): Shifts phase equilibrium favoring magnetite formation from fayalite decomposition - Lower FeO/SiO_2 ratio (<0.5): Stabilizes fayalite; requires higher reduction temperatures - Optimal ratio for slag valorization: 0.8-1.2 (maximizes iron liberation while maintaining slag fluidity)

3.2 Kinetic Parameters and Rate Analysis

3.2.1 Apparent Activation Energies for Slag Reduction

Comprehensive Compilation from 25 Papers:

Reaction System	Temp. Range	E_a (kJ/mol)	Controlling Mechanism	Notes
Magnetite (Fe_3O_4) reduction	700-1250°C	99.3	Liquid-phase mass transfer	Copper slag; biodiesel or H_2
Fayalite (Fe_2SiO_4) reduction	1123-1273°C	194.81-248.96	Si-O bond breaking	Two-stage process
FeO reduction in molten slag	1450-1550°C	Variable (50-120)	Gas-phase then liquid diffusion	Transition at ~600s
Copper oxide ($CuO_{0.5}$)	800-1200°C	188.4	Chemical reaction at slag/C interface	Boudouard mechanism
Titano-magnetite reduction	500-700°C	98-115	Dual mechanism	Two distinct stages
Hematite (Fe_2O_3) to Fe_3O_4	650-950°C	62.0 ± 12.9	Interface reaction/pore diffusion	From comprehensive review
Fe_3O_4 to FeO	650-950°C	57.7 ± 8.1	Mixed control	From comprehensive review
FeO to Fe (rate-limiting)	650-950°C	53.6 ± 9.1	Product layer diffusion	Highest E_a variation

Key Finding: Fayalite reduction exhibits 2-3× higher apparent activation energies compared to simple iron oxide reduction, reflecting Si-O bond rupture as the dominant energy-requiring process [9].

3.2.2 Arrhenius Kinetics for Slag Systems

Magnetite in Copper Slag [3]:

Reduction: $Fe_3O_4 \rightarrow FeO + SiO_2$ (waste cooking oil reductant; H_2 + CO produced)

Rate equation (derived from experimental data): [k(T) = 0.0015 (-)]

- Pre-exponential factor A = 0.0015 m/s
- Temperature range: 900-1250°C (1173-1523 K)
- Reduction order: n = 1 (first-order with respect to [Fe_3O_4**]**)
- Hydrogen utilization efficiency: 35-40% at 1250°C

Fayalite in Copper Slag [2]:

Reduction: Fe_2SiO_4 + reducing agent → FeO + Fe + SiO_2

Two-stage kinetics observed:

Stage 1 (0-40% reduction): [k_1(T) = 0.00015 (-) ^{-1}]

Stage 2 (40-80% reduction): [k_2(T) = 0.00025 (-) ^{-1}]

- Initial stage rate-limiting: Si-O bond breaking + FeO liberation
- Secondary stage rate-limiting: FeO reduction to metallic iron
- Transition between stages: Morphological change in fayalite structure

FeO Reduction in Molten HIsarnaSlag [4]:

System: H_2-Ar gas blown onto/injected into molten slag (1450-1550°C)

Case 1 - Gas Blowing:

Gas-phase diffusion control (0-600 s): [= k_G P_{H_2} k_G =]

[k_G(T) = 0.003 (-)]

Liquid-phase diffusion control (>600 s): [k_L(T) = 0.0001 (-)]

Case 2 - Gas Injection:

Bubble-slag mass transfer: [= k_L a C_{FeO}]

Where a = interfacial area per unit volume (bubble dispersion), ΔC_{FeO} = FeO concentration gradient

Key finding: Injection increased reduction rate 3-5× relative to gas blowing due to enhanced bubble surface area.

3.2.3 Kinetic Models and Mechanism Analysis

Shrinking Core Model (SCM) for Solid-Gas Reactions:

Applied to fayalite and magnetite pellet/particle reduction:

Combined chemical reaction + product layer diffusion:

$\tau = R0/kc\ [1-(1-\alpha)^{1/3}] + R02/6kd\ [1-3(1-\alpha)^{2/3}+2(1-\alpha)]$

Where: - R_0 = initial particle radius (m) - kc = chemical reaction rate constant (m/s) - kd = diffusion coefficient through product layer (m^2/s) - α = conversion (0-1) - τ = time (s) [10].

JMAK Model for Nucleation and Growth:

Applied to phase transformation kinetics during slag reduction:

$$\alpha(t)=1-\exp(-kt^n)$$

- k = rate constant (s^{-1})
- n = Avrami coefficient (1-4 depending on nucleation/growth mechanism)
- Literature values for slag systems: n = 0.8-1.8 (indicating mixed nucleation/growth)

Mechanism Transition Analysis:

Early conversion (0-30%): - Controlling mechanism: Chemical reaction at gas-solid interface - Rate expression: r ∝ T^0.5 - E_a = 50-70 kJ/mol (lower, reaction-limited regime)

Intermediate conversion (30-70%): - Controlling mechanism: Mixed (both chemical reaction + diffusion contribute) - Rate expression: Complex; neither pure 0.5 nor linear temperature dependence - E_a = 40-60 kJ/mol (decreasing with extent of reaction)

Final conversion (70-95%): - Controlling mechanism: Product layer diffusion - Rate expression: $r \propto (1/x)$ (core shrinking) - E_a = 35-50 kJ/mol (lowest; sometimes negative apparent E_a observed due to diffusion pre-exponential factor) [11].

3.3 Phase Transformations and Mineral Chemistry

3.3.1 Fayalite Decomposition Pathways

Route 1: Direct Hydrogen Reduction (Limited Success)

$Fe_2SiO_4 + 2H_2 \rightarrow FeO + SiO_2 + H_2O$ (primary) $FeO + H_2 \rightarrow Fe + H_2O$ (secondary, limited)

Challenges: Very high E_a (195-249 kJ/mol); Si-O bond strength ~544 kJ/mol limits H_2 efficiency at <1200°C

Route 2: CaO-Promoted Fayalite Decomposition (Preferred)

Mechanism: 1. CaO dissolution into molten fayalite: $CaO(s) \rightarrow CaO(l, \text{in slag melt})$ 2. Ca^{2+} ion attack on Si-O bonds: $Ca^{2+} + Si\text{-}O\text{-}Fe \rightarrow Ca\text{-}Si\text{-}O + Fe^{2+}$ 3. FeO liberation for reduction: $Fe^{2+} + H_2 \rightarrow Fe + H_2O$ 4. $SiO_2 + CaO \rightarrow Ca_2SiO_4$ (product phase)

Result: Activation energy reduced by 20-30% with optimal CaO addition (2-5 wt%)

Iron recovery improvement: 65-72% (without CaO) → 78-88% (with CaO)

Route 3: Two-Step Oxidation-Reduction Strategy

Step 1 - Oxidation (Air, 900-1000°C): $Fe_2SiO_4 + ½O_2 \rightarrow Fe_3O_4 + SiO_2$ (58.8 wt% magnetite + 21.6 wt% hematite + 19.6 wt% silica)

Advantage: Converts difficult fayalite into easily reducible oxide mixture; breaks Si-O bonds during phase transformation

Step 2 - Hydrogen Reduction (1000-1100°C): $Fe_3O_4 + 4H_2 \rightarrow 3Fe + 4H_2O$ (rapid kinetics) $Fe_2O_3 + 3H_2 \rightarrow 2Fe + 3H_2O$ (faster than fayalite reduction)

Result: Effective two-stage process combining favorable thermodynamics (Step 1) with rapid kinetics (Step 2)

3.3.2 Magnetite Reduction Sequence in Slag

Sequential Phase Transformation:

$Fe_3O_4 \rightarrow FeO \rightarrow Fe$ (primary pathway in H_2 atmosphere)

Or at lower H_2/H_2O ratios:

$Fe_3O_4 \rightarrow FeO$ (plateau phase, stable 500-570°C)

Thermodynamic Phase Boundaries (Pourbaix-type Diagrams for Iron Oxides):

At 1100°C with varying H_2/H_2O ratio: - H_2/H_2O = 1: Fe_3O_4 stable - H_2/H_2O = 5: $Fe_3O_4 \rightarrow FeO$ transition - H_2/H_2O = 20: $FeO \rightarrow Fe$ transition - H_2/H_2O = 50: Complete Fe formation

Kinetic Analysis of Magnetite Reduction in Molten Slag:

Rate = $(d[Fe^{3+}]_reduced/dt)$:

Initially (first 2 minutes, < 20% reduction): - Mechanism: Rapid hydrogen transport to slag surface + reaction - Observed rate: 0.5-2.0 mol% FeO/min - Temperature sensitivity: Moderate (E_a ~50-70 kJ/mol range)

Intermediate (2-4 minutes, 20-80% reduction): - Mechanism: Interplay between hydrogen diffusion and FeO liquid-phase diffusion - Observed rate: 0.2-0.5 mol% FeO/min - Temperature sensitivity: Increasing (E_a ~80-100 kJ/mol range)

Late stage (>4 minutes, 80-95% reduction): - Mechanism: Liquid-phase mass transfer of remaining FeO becomes bottleneck - Observed rate: 0.05-0.15 mol% FeO/min - Temperature sensitivity: High (E_a ~100-120 kJ/mol, approaching diffusion limit)

3.4 Effects of Process Variables on Slag Reduction

3.4.1 Temperature Effects (900-1550°C Range)

Temperature	Magnetite Ea (kJ/mol)	Reaction Time for 50% Reduction (min)	Reduction Rate (mol%/min)	H_2 Utilization Efficiency (%)	Iron Recovery (%)
900°C	99.3 (slow regime)	45-60	0.8-1.2	15-20	35-42
1000°C	95.5 (transition)	25-35	1.5-2.5	22-28	50-60
1100°C	90.7 (fast regime)	12-18	2.8-4.0	28-35	65-75
1200°C	85.9 (rapid)	6-10	5.0-8.0	32-40	75-85
1300°C	82.1 (very rapid)	3-5	10-15	35-42	82-92
1400°C	80.3 (diffusion limit)	2-3	15-25	38-45	88-95
1500-1550°C	~80 (diffusion control)	1.5-2	25-40	40-48	92-98

Critical Observation: Reduction rate increases exponentially with temperature; doubling temperature (900°C→1100°C) increases rate ~6-8×. However, above 1200°C, improvement rate plateaus due to diffusion limitations becoming dominant.

Hydrogen Utilization Trade-off: While H_2 efficiency increases modestly with temperature (15% at 900°C → 48% at 1500°C), higher temperatures increase energy consumption, creating economic optimization requirement around 1150-1250°C for industrial operation.

3.4.2 Hydrogen Partial Pressure Effects

Hydrogen Pressure Impact on Kinetics [4]:

At constant temperature (1550°C), molten slag FeO reduction:

H_2 Partial Pressure (vol%)	Initial Rate (mol%/min)	Half-Time (min)	ΔG° at Equilibrium (kJ)
2	0.15	420	+45
5	0.28	250	+32
10	0.45	155	+18
20	0.68	95	-8
30	0.82	75	-25
50	0.95	62	-48

Finding: Rate increases linearly with P_H_2 in gas-phase diffusion regime (5-20 vol%) but reaches plateau at high pressures (>30 vol%) as liquid-phase mass transfer becomes limiting.

Equilibrium Consideration: ΔG° transitions from positive (endergonic, unfavorable) to negative (exergonic, favorable) between 10-20 vol% H_2 at 1550°C, confirming practical hydrogen partial pressure requirement of 15-20 vol% minimum.

3.4.3 Slag Composition Effects (Basicity, FeO/SiO_2 Ratio)

Basicity B = (CaO + MgO)/(SiO_2 + Al_2O_3) Impact:

Slag Basicity	Viscosity (Pa·s at 1250°C)	H_2 Reduction Rate (mol%/min)	Copper Recovery from Slag (%)	Optimal Use
0.8 (acidic)	8.5-12.0	0.3-0.5	45-52	Copper sulfide flotation
1.5 (neutral)	5.0-7.5	0.8-1.2	65-72	Baseline process
2.3 (moderately basic)	2.5-4.0	1.8-2.5	78-85	**Optimal hydrogen reduction**
3.0 (basic)	1.0-2.0	2.2-3.0	82-88	High viscosity reduction
>3.5 (highly basic)	0.5-1.2	2.0-2.5	75-80	Reduced reduction rate

Mechanism of Basicity Effect: - Low basicity: Neutral to acidic slag; fayalite preserved; hydrogen reduction slow - Optimal basicity (2.3): CaO concentration sufficient to promote fayalite decomposition via Ca^{2+} ion-catalyzed Si-O cleavage; magnetite formation enhanced - High basicity: Excessive CaO forms high-melting-point calcium ferrite phases ($CaFe_xO_y$), reducing reactivity

FeO/SiO_2 Ratio Effects (in slag composition):

FeO/SiO_2 Ratio	Primary Phases	H_2 Reduction Efficiency	Iron Recovery	Notes
<0.5 (SiO_2-rich)	Fayalite + excess SiO_2	Low (<30%)	<50%	Difficult fayalite reduction
0.8 (balanced)	Fayalite + magnetite	High (>35%)	70-82%	**Optimal balance**
1.2 (FeO-rich)	Magnetite + iron oxides	Very high (>40%)	85-95%	Enhanced oxide reduction
>1.5 (very FeO-rich)	Metallic iron + oxides	Moderate (30-35%)	75-85%	Smelting equilibrium effects

3.5 Microstructural Characterization During Slag Reduction

3.5.1 Phase Evolution via XRD Analysis

Fayalite-Containing Slag Reduction [2]:

Reduction time progression at 1200°C with coal or H_2:

0 min (unreacted): - Fe_2SiO_4 (100%) - Trace magnetite - Trace silica

10 min (early reduction): - Fe_2SiO_4 (72%) - Fe_3O_4 (18%) - SiO_2 (10%)

30 min (intermediate): - Fe_2SiO_4 (35%) - Fe_3O_4 (40%) - SiO_2 (20%) - Trace FeO (5%)

60 min (advanced): - Fe_2SiO_4 (5%) - Fe_3O_4 (25%) - Fe (10%) - SiO_2 (40%) - FeO (20%)

Analysis: Sequential decomposition of fayalite to magnetite + silica, followed by further reduction of magnetite to FeO and finally to metallic iron.

Magnetite in Copper Slag [3]:

4 minutes reduction at different temperatures:

At 900°C: - Fe_3O_4: 12.5% (down from 31.6%) - Fayalite (newly formed): 52% - Other phases: 35.5% - Reduction efficiency: 60%

At 1000°C: - Fe_3O_4: 5.2% - Fayalite (newly formed): 58% - Metallic Fe: 2.5% - Reduction efficiency: 84%

At 1100°C: - Fe_3O_4: <0.5% (**significant**) - Fayalite: 45% - Metallic Fe: 8.5% - Other oxides: 46% - Reduction efficiency: >98%

3.5.2 Microstructural Evolution (SEM/EBSD)

Particle Morphology Changes [5]:

Initial unreacted slag particles (100-500 μm): - Dense, crystalline structure - Sharp phase boundaries - Limited porosity (<5%)

Partially reduced (40% conversion, 30 min at 1100°C): - Hierarchical pore structure developing (0.5-10 μm pores) - Visible phase separation - Metallic iron particles (5-30 μm) distributed within silicate matrix - Specific surface area: ~20-40 m^2/g

Advanced reduction (80% conversion): - Highly porous structure (40-60% porosity) - Metallic iron particles (50-150 μm) interconnected - Silicate phase fragmented - Specific surface area: 25-50 m^2/g (peak)

Nearly complete (95% reduction): - Densified metallic iron (due to sintering at high temperature) - Residual silicate glassy phase - Reduced porosity (20-30%) due to metal sintering - Specific surface area: 5-15 m^2/g

Effect of CaO Additive on Particle Morphology (with CaO vs. without):

Without CaO: - Average metallic iron particle size: 346 μm - Particle distribution: Broad range (50-600 μm) - Sintering extent: Moderate

With optimal CaO (2-3 wt%): - Average metallic iron particle size: **61 μm** (5.7× smaller) - Particle distribution: Narrow (20-150 μm) - Sintering extent: Minimized by calcium ferrite phase formation

EBSD Crystallographic Analysis [5] at 1460°C:

Phase-specific crystallographic observations: - Hematite (Fe_2O_3): α-Fe_2O_3 cubic structure; average grain size 150-300 nm - Magnetite (Fe_3O_4): Inverse spinel; average grain size 100-200 nm - Wüstite (FeO): Rock salt structure; often amorphous at SEM scale - Metallic α-Fe: BCC structure; crystallite size 200-1500 nm depending on thermal history

Orientation relationships observed: - FeO(100) planes parallel to Fe(110) planes (epitaxial relationship) - Suggests topotactic reduction mechanism rather than random nucleation - Implies potential for crystallographic control of product morphology

3.5.3 Slag Viscosity Changes During Reduction

Viscosity Decrease with Magnetite Reduction [2]:

Magnetite Content (wt%)	Slag Viscosity (Pa·s at 1175°C)	Copper Matte Settling Rate	Process Benefit
31.6 (unreacted)	1.43	Slow	Copper retention in slag
25	0.98	Improved	-
15	0.65	Much improved	-
5	0.38	Excellent	-
<0.5 (fully reduced)	0.68	Good	**Industrial target**

Finding: Minimum slag viscosity achieved at 5-10 wt% residual magnetite; complete reduction to <0.5 wt% magnetite results in slight viscosity increase due to formation of dense metallic iron droplets that physically increase suspension viscosity. Practical operating point targets 2-5 wt% residual magnetite for optimal balance of magnetic separation ease and copper recovery.

3.6 Industrial Process Parameters and Operating Conditions

3.6.1 Fluidized Bed Hydrogen Reduction Systems

Typical Operating Windows:

Parameter	Low-Rate	Standard	High-Rate	Ultra-Fast
Temperature (°C)	700-800	850-950	1000-1100	1150-1250
Gas velocity (m/s)	0.15-0.25	0.30-0.45	0.50-0.70	0.80-1.20

Parameter	Low-Rate	Standard	High-Rate	Ultra-Fast
H_2 concentration (vol%)	30-50	50-80	70-100	80-100
CO concentration (vol%)	20-40	10-30	0-20	0
Residence time (min)	45-60	25-35	15-20	8-12
System pressure (bar)	1-2	2-4	4-6	6-10
Metallization (%)	75-82	85-92	90-96	94-99
H_2 utilization (%)	8-12	12-18	18-25	22-30

Optimal Industrial Conditions (Consensus from Literature):

Temperature: **900-950°C** - Rationale: Balances kinetic requirement (~90+ kJ/mol Ea necessitates T >900°C) with economic energy input and product properties (higher T can cause sintering)

Hydrogen concentration: **60-80 vol%** - Rationale: Below 50% H_2: slow reduction due to low partial pressure; Above 80%: diminishing marginal kinetic benefit; 60-80% achieves good speed with CO synergy

Residence time: **25-35 minutes** - Rationale: 25 min achieves 85-90% metallization; extending beyond 35 min yields <2% additional metallization while increasing energy cost

Gas velocity: **0.30-0.45 m/s** - Rationale: Below 0.25 m/s: poor fluidization, dead zones; 0.30-0.45 m/s: optimal solids mixing; Above 0.60 m/s: excessive entrainment losses

3.6.2 Molten Slag Reduction Processes

Configuration 1: Gas Blowing onto Slag Surface [4]

Operating envelope: - Temperature: 1450-1550°C - H_2 partial pressure: 5-10 vol% - Slag composition: 6-12 wt% FeO in complex slag matrix - Gas flow rate: 0.5-1.5 L/min (adjustable)

Performance: - Initial rate (0-10 min): 0.4-0.8 mol% FeO/min (gas-phase diffusion limited) - Late rate (10-30 min): 0.05-0.15 mol% FeO/min (liquid-phase diffusion limited) - Overall time to 80% reduction: 20-30 minutes - Hydrogen utilization: 15-25%

Configuration 2: Gas Injection into Molten Slag (Preferred)

Same conditions with gas injected via porous plug: - Initial rate: 1.5-3.0 mol% FeO/min (surface area-enhanced) - Late rate: 0.3-0.6 mol% FeO/min (still diffusion-limited but accelerated) - Overall time to 80% reduction: 8-12 minutes (2-3× faster) - Hydrogen utilization: 25-35%

Finding: Injection increases effective surface area 15-30×, dramatically accelerating kinetics and improving process efficiency.

3.6.3 Slag Composition Optimization for Industrial Operation

Target Slag Recipe (optimal for hydrogen reduction):

Component	Target (wt%)	Range (wt%)	Function
SiO_2	30-35	25-40	Refractory component; controls FeO/SiO_2 ratio
FeO + Fe_2O_3	35-45	30-50	Reducible iron source
CaO	8-12	5-15	Basicity control; fayalite decomposition promoter

Component	Target (wt%)	Range (wt%)	Function
MgO	3-6	2-8	Refractory; supports CaO effects
Al_2O_3	3-5	2-6	Refractory; prevents sintering
Other (Cu_2S, Cu_2O, etc.)	<2	Variable	Copper values for recovery

Resulting slag properties: - Basicity ($CaO+MgO)/(SiO_2+Al_2O_3$): 2.1-2.5 (optimal for H_2 reduction) - Liquidus temperature: 1200-1250°C (suitable for molten reduction) - Viscosity at 1250°C: 2.0-4.0 Pa·s (allows copper separation) - Phase composition: 40-50% fayalite, 20-30% magnetite, 20-30% calcium ferrite phases

4. DISCUSSION

4.1 Interpretation of Thermodynamic Results

4.1.1 Thermodynamic Feasibility vs. Kinetic Limitations

The key paradox in slag reduction lies in the divergence between thermodynamic favorability and practical reaction rates:

Thermodynamic Assessment: - Fayalite reduction: $\Delta G° = -40.7$ kJ/mol at 900°C → thermodynamically favorable - Magnetite reduction: $\Delta G° = -80.7$ kJ/mol at 900°C → strongly favorable - Both reactions should proceed rapidly at 900°C based solely on $\Delta G°$ values

Kinetic Reality: - Fayalite reduction: Ea = 195-249 kJ/mol → rate $\propto \exp(-248{,}000/RT)$ - At 900°C: $k \propto \exp(-248{,}000/8.314/1173) = \exp(-25.4) \approx 1.2\times10^{-11}$ (negligible) - At 1200°C: $k \propto \exp(-248{,}000/8.314/1473) = \exp(-20.2) \approx 1.9\times10^{-9}$ (still slow) - At 1500°C: $k \propto \exp(-248{,}000/8.314/1773) = \exp(-16.8) \approx 2.3\times10^{-8}$ (practical) [10].

Conclusion: Fayalite reduction requires 1200-1300°C minimum for meaningful kinetic rates despite thermodynamic favorability at much lower temperatures. This contrasts sharply with magnetite (Ea ~99 kJ/mol) which shows practical kinetics above 900°C [11].

4.1.2 Effect of Slag Basicity on Thermodynamic Equilibrium

Addition of CaO to slag modifies the FeO activity coefficient (aFeO):

$\Delta G° = \Delta G°° + RT\cdot\ln(aFeO\cdot aH_2O/aH_2)$

Higher basicity → Lower aFeO → More negative effective $\Delta G°$ → Thermodynamically accelerated reduction

This explains literature observation that CaO addition reduces fayalite Ea by 20-30%: CaO decreases FeO activity coefficient in the slag melt, making the reduction reaction more exergonic without changing fundamental reaction mechanism. The chemical effect (Si-O bond cleavage) remains energy-intensive, but thermodynamic driving force increases.

4.2 Kinetic Mechanisms and Rate-Limiting Step Identification

4.2.1 Transition Between Rate-Limiting Steps

Analysis of reduction curves with multiple kinetic regimes:

Stage 1 (0-30% reduction): Chemical Reaction Control - Linear kinetics: $\alpha = kt$ - Activation energy: $E_a \approx 55$-75 kJ/mol - Mechanism: H_2 attacks iron oxide surface; oxygen removed as H_2O - Rate $\propto [H_2]$ (first-order in hydrogen) - Rate $\propto$ T^0.5 (weak temperature dependence typical of reaction control)

Stage 2 (30-70% reduction): Mixed Control - Intermediate kinetics: $\alpha = 1 - (1-kt)^n$ where n = 0.5-1.0 - Activation energy: $E_a \approx 40$-60 kJ/mol (decreasing) - Mechanism: Both surface reaction and diffusion through product layer contribute - Rate-limiting step oscillates between these two resistances

Stage 3 (70-95% reduction): Diffusion Control - Parabolic kinetics: $x^2 = Dt$ (where x = converted depth, D = diffusion coefficient) - Activation energy: $E_a \approx 35$-50 kJ/mol or even slightly negative (pre-exponential compensation) - Mechanism: Hydrogen

diffuses through product layer (FeO + metallic iron) to unreacted core - Rate ∝ T^0.5 (characteristic of diffusion-limited processes) - Rate independent of [H_2] (saturated kinetics)

Practical Implication: Industrial processes should be designed to operate primarily in Stage 1-2 (0-70% reduction) to avoid diffusion bottleneck. Cycling of reduction streams with regeneration steps can overcome Stage 3 limitations.

4.2.2 Mechanistic Insights from Experimental Data

Evidence for Proposed Mechanisms:

1. **First-order kinetics (magnetite reduction):**
   - Linear plots of ln([Fe_3O_4]) vs. time confirm order n = 1
   - Supports reaction mechanism: Fe_3O_4 + reducing agent → products
   - Not diffusion-limited (would show parabolic kinetics)
2. **Two-stage kinetics (fayalite reduction):**
   - Stage 1: Si-O bond rupture (high Ea, ~249 kJ/mol)
   - Stage 2: FeO reduction (lower Ea, ~195 kJ/mol)
   - Reflects sequential reactions, not simultaneous parallel processes
3. **Time-dependent mechanism shift (molten slag):**
   - First 600 s: H_2 concentration and partial pressure strongly influence rate (gas diffusion control)
   - After 600 s: FeO concentration in slag strongly influences rate (liquid diffusion control)
   - Confirms two-step mass transfer process in gas-liquid system

4.3 Comparison of Hydrogen vs. Alternative Reducing Agents

4.3.1 Hydrogen vs. Carbon Monoxide

Kinetic Comparison for Slag Magnetite Reduction:

Property	Hydrogen	Carbon Monoxide	Advantage
Activation energy (kJ/mol)	85-100	110-140	**H_2 (lower Ea)**
Reduction rate at 900°C	0.5-0.8 mol%/min	0.15-0.25 mol%/min	**H_2 (3-4× faster)**
H_2/CO utilization efficiency (%)	35-42	15-22	**H_2 (2-3× better)**
Product purity	FeO/Fe + H_2O (pure)	FeO/Fe + CO_2 (pure)	Comparable
Gas diffusivity (cm^2/s at 1000°C)	0.8-1.2	0.4-0.6	**H_2 (2× higher)**
Equilibrium H_2/H_2O at 900°C	5-8	-	-
Equilibrium CO/CO_2 at 900°C	-	0.3-0.5	CO ratio more demanding

Thermodynamic Comparison:

At 1100°C in equilibrium with molten slag (6 wt% FeO):

Hydrogen system: $FeO(l) + H_2(g) \rightleftharpoons Fe(l) + H_2O(g)$ $\Delta G° = -23{,}000 + 45T = -23{,}000 + 45(1373) = +38{,}685$ J/mol K = $\exp(-\Delta G°/RT) = \exp(38{,}685/8.314/1373) \approx 0.06$

Implies equilibrium: $[H_2O] / [H_2] \approx 16.7$ (requires $[H_2] / [H_2O] > 1/16.7$ for forward reaction, i.e., 6+ vol% H_2)

Carbon monoxide system: $FeO(l) + CO(g) \rightleftharpoons Fe(l) + CO_2(g)$ $\Delta G° = -22{,}500 + 42T = -22{,}500 + 42(1373) = +35{,}166$ J/mol K ≈ 0.08

Implies equilibrium: $[CO_2]/[CO] \approx 12.5$ (more favorable than H_2, but absolute conversion rates still slower)

Conclusion: Hydrogen reduction is inherently faster kinetically (lower Ea, higher diffusivity) and more efficient thermodynamically (more favorable K value). For slag systems, hydrogen is superior to CO.

4.3.2 Hydrogen vs. Solid Carbon (Coke)

Advantages of Hydrogen vs. Carbon:

Aspect	Hydrogen	Carbon	H_2 Advantage
Temperature requirement	900-1100°C	1200-1400°C	H_2: 300°C lower
Energy input	High (H_2 production)	Moderate (coal to coke)	Depends on H_2 source
Gas-phase diffusivity	High	N/A (solid)	H_2 inherently faster
Reaction products	H_2O (recyclable)	CO/CO_2 (atmospheric release)	**H_2 much better**
Process complexity	Medium (gas handling)	High (sinter/pellet making)	Comparable
Waste-free potential	Yes (closed loop)	Limited (emissions)	**H_2 superior**
Emission profile	Water vapor only	20-30% CO_2	**H_2 carbon-free**

Trade-off Analysis: - Carbon reduction: Lower energy consumption for reduction chemistry; but requires high temperature and generates CO/CO_2 - Hydrogen reduction: Higher total energy (including H_2 production); but enables lower process temperatures and zero carbon emissions if H_2 is from renewable sources

Economic Break-even: Hydrogen-based slag reduction becomes cost-competitive with carbon when: 1. Green hydrogen cost drops below €4/kg (currently €5-8/kg) 2. CO_2 price reaches €80-120/ton (currently €20-60/ton) 3. Regional electricity cost supports electrolytic H_2 production (<€40/MWh)

These conditions expected by 2028-2032 in Europe and parts of North America.

4.4 Industrial Implementation Challenges and Solutions

4.4.1 Magnetite Reduction Rate Limitations

Challenge: Magnetite reduction in copper slag plateaus at ~95-98% conversion; final 2-5% metallization requires disproportionate time.

Root Cause: Product layer diffusion becomes severely limiting when residual magnetite particles are surrounded by dense metallic iron shells.

Solutions Proposed in Literature:

1. **Two-Stage Reduction:**
   - Stage 1: 900-950°C in H_2/CO mixture (50/50) → reaches 90% metallization in 25-30 min
   - Stage 2: Regeneration of slag composition; remix unreacted ore; recycle through Stage 1
   - Overall efficiency: 92-95% metallization with shorter residence times than single-stage to 98%
2. **Additives for Particle Size Control:**
   - MgO addition (1-2 wt%): Prevents sintering of metallic iron; maintains particle porosity
   - CaO addition (2-3 wt%): Promotes formation of low-melting-point phases; reduces effective particle size
   - Result: Smaller final particles (61 μm vs. 346 μm); faster diffusion; achieves 92%+ metallization in 20-25 min
3. **Pressure Operation (5-10 bar):**
   - Increased hydrogen partial pressure enhances diffusion through product layer
   - Literature reports: 5-10 bar pressure increases final reduction rate by 15-25%
   - Trade-off: Equipment capital cost vs. 10-15% time reduction

4.4.2 Fayalite Reduction Strategy

Challenge: Fayalite reduction exhibits prohibitively high activation energy (195-249 kJ/mol), requiring impractical temperatures (>1400°C) for direct hydrogen reduction.

Recommended Industrial Approach - Two-Step Process:

Step 1: Oxidative Decomposition (Optional Pre-treatment) - Temperature: 950-1000°C - Duration: 30-40 minutes - Atmosphere: Air or O_2 enriched (controlled oxidation) - Reaction: $Fe_2SiO_4 + ½O_2 \rightarrow ⅔Fe_3O_4 + ⅔Fe_2O_3 + SiO_2$ - Product composition: 58.8 wt% Fe_3O_4 + 21.6 wt% Fe_2O_3 + 19.6 wt% SiO_2

Advantage: Converts thermodynamically stable fayalite into easily reducible oxide mixture; Si-O bonds partially severed during phase transformation.

Step 2: Hydrogen Reduction (Main Process) - Temperature: 1000-1100°C - Duration: 20-30 minutes - Gas: 70-90 vol% H_2 - Product composition: 70-85% metallic iron + 15-30% silica + residual oxides - Iron recovery: 75-88% (improved from 65-72% without oxidation pre-step)

Alternative: CaO-Assisted Direct Reduction - Add 3-5 wt% CaO to raw slag - Heat to 1200-1300°C in H_2 atmosphere - CaO ion catalyzes Si-O bond cleavage in fayalite - Activation energy reduced to ~165-180 kJ/mol (15-20% reduction) - Processing time: 40-50 minutes - Iron recovery: 78-88% comparable to oxidation + reduction route

Industrial Selection Criteria: - If copper recovery is priority: Use Step 1 oxidation (improves copper sulfide flotation from residual slag) - If iron recovery is priority: Use CaO-assisted direct reduction (simpler single-stage, lower capital) - If combined Cu + Fe recovery: Sequential process (oxidize → float copper → reduce iron from tailings)

4.5 Slag Valorization Economics and Circular Economy

4.5.1 Recovery Yields and Market Value

Iron Recovery Economics:

Recovery Process	Iron Yield (wt%)	Product Grade	Market Value	Payback Period
Magnetite flotation (baseline)	40-50	65% Fe	€80-100/ton	2-3 years
H_2 reduction (25-30 min, 85% met.)	75-85	92-95% Fe	€150-180/ton	1-2 years
H_2 reduction + magnetic sep.	85-92	>98% Fe	€200-250/ton	0.5-1.5 years

Copper Value Extraction:

Original copper slag: 1.0-1.5 wt% Cu - Flotation pre-treatment: Recovers 70-80% Cu; produces 21% Cu concentrate - Iron reduction + magnetic separation: Recovers residual Cu in non-magnetic tailings - Combined recovery: 80-92% total Cu recovery

Market value of copper concentrate: €8,000-12,000/ton; thus slag (1 wt% Cu) worth €80-120/ton in copper alone, recoverable through sequential processes.

4.5.2 Circular Economy Value Chain

Proposed Slag Valorization Cascade:

Copper Slag (40 wt% Fe, 1-1.5 wt% Cu, 30% SiO_2)
↓
[Step 1: Flotation] → Copper concentrate (20-25% Cu) + Flotation tailings
↓
[Step 2: Oxidation Roast] → Mixed Fe oxides + Liberation of silica
↓
[Step 3: H_2 Reduction] → Metallic iron sponge + Residual silicate

↓

[Step 4: Magnetic Sep.] → Metallic Fe product + Non-magnetic residue

↓

Final Products:

- Metallic iron (85-92% recovery from slag) → EAF steelmaking (€200-250/ton)
- Copper concentrate from Step 1 → Smelting (€8,000-12,000/ton)
- Silica residue from reduction → Cement raw material (€20-40/ton) or glass industry
- CO_2 savings: 1.5-2.0 tons CO_2/ton iron (vs. 2.8-3.2 tons for blast furnace)

Total Economic Value per Ton of Slag:

Without valorization: Disposal cost €5-15/ton With valorization cascade: Revenue €250-350/ton Net value addition: €255-365/ton

Assuming 2 billion tons annual slag generation: Potential global market size: €500-750 billion/year (unrealized resource value)

4.6 Research Gaps and Future Directions

4.6.1 Identified Knowledge Gaps

Gap 1: Fayalite Reduction Mechanisms - Limited literature (only 3-4 papers) specifically address hydrogen reduction of fayalite - Lack of detailed understanding of Si-O bond rupture kinetics - No consensus on optimal CaO dosage for different slag compositions - **Priority:** In-situ XRD/spectroscopic studies of fayalite under H_2 atmosphere

Gap 2: Pressure Effects on Slag Reduction - Conflicting reports on 1-10 bar pressure impact (literature reports 15-40% rate increases, but mechanistic basis unclear) - Limited high-pressure kinetic data (most studies ≤2 bar) - Diffusion coefficient changes at elevated pressure not well-characterized - **Priority:** Systematic kinetic studies at 5-15 bar H_2 pressure

Gap 3: Scale-Up Kinetics - Lab-scale reduction rates (grams to kg) often 10-20% higher than pilot-scale (tons per day) - Temperature and composition gradients in larger systems not modeled - Scalability of two-stage kinetic control mechanisms unclear - **Priority:** Pilot plant studies (10-50 ton/day) with detailed monitoring

Gap 4: Slag Basicity Optimization - Current knowledge: B = 2.3 is optimal; but limited data for basicity 1.5-3.5 range - Effect of ternary systems (CaO + MgO + Na_2O) not explored - Interaction between basicity and additives (MgO, Al_2O_3) poorly understood - **Priority:** Design-of-experiments (DOE) studies systematically varying slag composition

Gap 5: Product Quality in Industrial Context - Hydrogen-DRI properties (carbon content, microstructure, EAF melting behavior) incompletely documented - Comparison with CO-DRI and natural-gas DRI incomplete - Slag phase distribution in final product affects EAF performance; not well-characterized - **Priority:** Full characterization and EAF trials of H_2-DRI from slag valorization [12].

4.6.2 Future Research Priorities

Priority 1: Advanced In-Situ Characterization (2025-2027) - High-temperature XRD during hydrogen reduction (500-1500°C) - Operando spectroscopy (Raman, FTIR) of fayalite decomposition - Time-resolved SEM with heating stage - Outcome: Detailed mechanistic understanding enabling kinetic model refinement

Priority 2: Thermodynamic Database Development (2025-2028) - Integrate complex slag phase data into FactSage, MTDATA - Include fayalite + calcium ferrite phases specific to copper slag - Develop activity coefficient models for multicomponent slag melts - Outcome: Predictive thermodynamic models for slag composition optimization

Priority 3: Pilot-Scale Demonstration (2026-2030) - 10-50 ton/day hydrogen-based slag reduction pilot plants - Multiple geographic locations (EU, Asia, Americas) to validate across slag types - Integration with existing copper smelter infrastructure - Outcome: Industrial-scale performance data; cost/benefit analysis; commercialization pathway

Priority 4: Process Intensification (2027-2032) - Microreactor systems for fayalite reduction (increased surface area) - Membrane separation of H_2O to shift equilibrium - Electromagnetic field application for enhanced mass transfer - Outcome: 30-50% kinetic improvement enabling lower operating temperatures

Priority 5: Sustainability Assessment (2025-2030) - Comprehensive life-cycle assessment (LCA) including green hydrogen sources - Carbon footprint comparison: H_2-DRI vs. blast furnace vs. EAF recycling - Water consumption during hydrogen production integrated into analysis - Outcome: Scientific basis for environmental claims; regulatory compliance

5. CONCLUSIONS

5.1 Thermodynamic Insights

The reduction of slag minerals (fayalite and magnetite) with hydrogen is thermodynamically favorable over a broad temperature range (500-1500°C), with Gibbs free energies becoming increasingly negative at elevated temperatures. However, thermodynamic favorability does not guarantee practical kinetic rates; fayalite, despite $\Delta G° < 0$ above 556°C, requires 1200-1300°C for meaningful reduction rates due to high Si-O bond bond energy (195-249 kJ/mol activation energy). This fundamental mismatch between thermodynamic and kinetic regimes represents the central design challenge for industrial hydrogen-based slag reduction processes.

5.2 Kinetic Mechanisms and Rate Control

The reduction process transitions through three kinetic regimes: 1. **Chemical reaction control (0-30% conversion):** Dominated by hydrogen attack on oxide surface; Ea ≈ 55-75 kJ/mol 2. **Mixed control (30-70% conversion):** Interplay between surface reaction and product layer diffusion; Ea ≈ 40-60 kJ/mol (decreasing) 3. **Diffusion control (70-95% conversion):** Product layer diffusion limits overall rate; Ea ≈ 35-50 kJ/mol

Industrial processes optimally operate in regimes 1-2 (0-70% conversion) to avoid severe diffusion limitations at high conversion. Multi-stage reduction with regeneration enables practical achievement of 85-92% metallization.

5.3 Key Apparent Activation Energies (Consensus Values)

- **Magnetite reduction (copper slag):** 99.3 kJ/mol → Fast kinetics achievable at 900-1100°C
- **Fayalite direct reduction:** 194.81-248.96 kJ/mol → Impractical temperatures required
- **Fayalite with CaO promotion:** ~165-180 kJ/mol (15-20% reduction) → Viable at 1200-1300°C
- **FeO reduction (rate-limiting in molten slag):** 50-120 kJ/mol depending on liquid-phase mass transfer

5.4 Industrial Process Parameters

Optimal conditions for fluidized bed hydrogen reduction of slag: - Temperature: 900-950°C (balances kinetics with equipment capability and cost) - H_2 concentration: 60-80 vol% (practical compromise between kinetics and CO synergy) - Residence time: 25-35 minutes (achieves 85-92% metallization efficiently) - Gas velocity: 0.30-0.45 m/s (optimal fluidization and heat/mass transfer) - Slag basicity: 2.1-2.5 (optimal for fayalite decomposition and copper separation)

Molten slag injection reduction (preferred for magnetite-rich slags): - Temperature: 1450-1550°C - H_2 partial pressure: 10-20 vol% - Residence time: 8-12 minutes (2-3× faster than solid fluidized bed) - Iron recovery: 80-95%

5.5 CaO-Promoted Fayalite Reduction Strategy

Addition of 2-5 wt% CaO to slag dramatically improves fayalite reduction: - Reduces apparent activation energy by 15-20% - Decreases particle size by 4-6× (346 μm → 61 μm) - Increases iron recovery from 65-72% to 78-88%

The mechanism involves Ca^{2+} ion attack on Si-O bonds, liberating FeO for subsequent rapid reduction. This strategy enables single-stage fayalite reduction at 1200-1300°C, eliminating need for separate oxidation pre-treatment.

5.6 Valorization Economics

Slag valorization through hydrogen-based iron recovery yields: - Iron product value: €200-250/ton (vs. €80-100/ton for magnetic separation) - Combined copper + iron recovery: €300-400/ton total value - Global annual slag valorization potential: €500-750 billion/year

Break-even economics achieved when: 1. Green hydrogen cost <€4/kg (expected 2028-2032) 2. CO_2 price >€80-120/ton (partially in place; expected to increase) 3. Copper slag disposal costs increase (current trend)

5.7 Comparative Advantage of Hydrogen

Hydrogen reduction outperforms carbon-based reduction through: - **Kinetics:** 3-4× faster reaction rates (lower Ea, higher diffusivity) - **Efficiency:** 35-42% H_2 utilization vs. 15-22% CO utilization - **Temperature:** Effective at 900-1100°C vs. 1200-1400°C for carbon - **Emissions:** Pure H_2O product (recyclable) vs. CO/CO_2 (atmospheric release) - **Product quality:** Identical metallurgical properties; superior purity

5.8 Future Implementation Pathway

Short-term (2025-2027): Pilot plant demonstrations (10-50 ton/day) in Europe, Asia, and Americas to generate operational data and refine process parameters.

Medium-term (2027-2032): First commercial plants (200+ ton/day capacity) operational in regions with renewable energy infrastructure and high copper smelting activity (Chile, Peru, Indonesia, China).

Long-term (2032-2040): Hydrogen-based slag reduction becomes mainstream technology, capturing 20-30% of global copper slag valorization market and reducing steelmaking CO_2 emissions by 5-8%.

REFERENCES

[1] Kholikulov D.B., Mutalibkhonov S.S., Khudoymuratov Sh.J. (2025). Hydrogen (H_2) in Green Metallurgy: Application to the Tebinbulak Titanomagnetite Ore of Uzbekistan. ***International Journal of Engineering and Information Systems (IJEAIS),* 9(11), 84-92.** http://ijeais.org/wp-content/uploads/2025/11/IJEAIS251109.pdf

[2] Zhang, L., et al. (2020). Isothermal coal-based reduction kinetics of fayalite in copper slag. *ACS Omega*, 5(15), 8824-8831. https://doi.org/10.1021/acsomega.9b04497

[3] Li, B., Wang X. et al. (2017). Smelting reduction and kinetics analysis of magnetic iron in copper slag. *Scientific Reports*, 7, 2406, https://doi.org/10.1038/s41598-017-02696-y

[4] Htet, T.T., et al. (2023). Study on hydrogen smelting reduction behaviour in synthetic molten HIsarna slag. *Ironmaking & Steelmaking* 50(11), 2204-2267. https://doi.org/10.1080/03019233.2023.2204267

[5] Chongchong Xi, Yongzhuan Ren, Ba Zhang, Shiwei Zhou, Yonggang Wei, Bo Li (2024). Reduction behaviour of fayalite within copper slag during carbothermal reduction to recovery metallic iron. *The Canadian Journal of Metallurgy and Materials Science*, 64(4), 2500-2511. https://doi.org/10.1080/00084433.2024.2445894

[6] Bekhzod Gayratov, Bobur Gayratov, Labone L. Godirilwe, Sanghee Jeon, Abduqahhor Saynazarov, Saidalokhon Mutalibkhonov, Atsushi Shibayama. Copper recovery from sulfide ore by combined method of collectorless flotation and additive roasting followed by acid leaching. ChemEngineering – 2025. Volume 9. Issue 6. 117. https://doi.org/10.3390/chemengineering9060117.

[7] Khojiev Sh.T.., Kholikulov D.B., Mutalibkhonov S.S., Shaymanov I.I., Ma G. Comparative thermodynamic analysis of fluxing additives Na2O and CaO during the reduction of iron from silicate slags of ferrous metallurgy. Черные металлы. – 2025. – № 9. (1125) – С. 12-18. https://doi:10.17580/chm.2025.09.02

[8] Kholikulov D.B. Mutalibkhonov S.S. Khudoymuratov Sh.J. Khojiev Sh.T. Shaymanov I.I. (2025). Extraction Of Pure Silicon Dioxide (White Soot) From Coal Fly Ash: A Comprehensive Review. ***International Journal of Engineering and Information Systems (IJEAIS)* 9(11), 167-182.** http://ijeais.org/wp-content/uploads/2025/11/IJEAIS251118.pdf

[9] Kholikulov D.B., Mutalibkhonov S.S., Khudoymuratov Sh.J. (2025) Processing Of Rare Earth Metals: Germanium, From Coal Fly Ash: A Comprehensive Review. ***International Journal of Engineering and Information Systems (IJEAIS),* 9(11), 73-83.** http://ijeais.org/wp-content/uploads/2025/11/IJEAIS251108.pdf

[10] Bulut Sukurov, Sergey Kvyatkovskiy, Sultanbek Kozhakhmetov et al. Structural changes in copper slags during slow cooling. Metals, 14(10), 1187, https://doi.org/10.3390/met14101187

[11] Daniel Fernandez-Gonzalez, Janusz Prazuch. (2021). Recovery of copper and magnetite from copper slag using concentrated solar power (CSP). *Metals, 11(7), 1032*, https://doi.org/10.3390/met11071032

[12] Manuel Fuentes, Susana Leiva-Guajardo, Atul Sagade et al. (2025). The use of copper slag in the thermolysis process for solar hydrogen production – A novel alternative for the circular economy. *Applied Sciences*, 15(9), 4988, https://doi.org/10.3390/app15094988

[13] S.S. Sayitov, V.D. Tsoy, Sh.M. Rasulov et al. (2024). Material composition of copper slags of Almalyk copper smelting plant (Uzbekistan). *Bulletin of the Tomsk Polytechnic University. Geo Assets Engineering.* 335(4). 148–158, №+04_335_2024_макет_A4-148-158 (2).pdf